The U.S. GOVERNMENT

IS ABSOLVED

FROM ANY LITIGATION WHICH MAY

ENSUE FROM THE CONTRACTORS IN-

FRINGING ON THE FOREIGN PATENT

RIGHTS WHICH MAY BE INVOLVED.

WRIGHT FIELD, DAYTON, OHIO

REEL – C

204

A.T.I.

7241

UNCLASSIFIED

NATIONAL ADVISORY COMMITTEE FOR AERONAUTICS

TECHNICAL NOTE

No. 1187

FORMULAS FOR ADDITIONAL MASS CORRECTIONS TO THE MOMENTS OF INERTIA OF AIRPLANES

By Frank S. Malvestuto, Jr. and Lawrence J. Gale

Langley Memorial Aeronautical Laboratory
Langley Field, Va.

Washington
February, 1947

NATIONAL ADVISORY COMMITTEE FOR AERONAUTICS

TECHNICAL NOTE NO. 1187

FORMULAS FOR ADDITIONAL-MASS CORRECTIONS

TO THE MOMENTS OF INERTIA OF AIRPLANES

By Frank S. Malvestuto, Jr. and Lawrence J. Gale

SUMMARY

Formulas are presented for the calculation of the additional-mass corrections to the moments of inertia of airplanes. These formulas are of particular value in converting the virtual moments of inertia of airplanes or models experimentally determined in air to the true moments of inertia. A correlation of additional moments of inertia calculated by these formulas with experimental additional moments of inertia obtained from vacuum-chamber tests of 40 spin-tunnel models indicates that the formulas give satisfactory estimations of the additional moments of inertia.

INTRODUCTION

In stability investigations involving free-flight tests of dynamically scaled models or of full-scale airplanes it is necessary to know accurately the true moments of inertia of the model or airplane. In order to obtain the true moments of inertia of the model or airplane the experimental moments of inertia, determined by the pendulum method, must be corrected for the effect of the surrounding air. The effect of this ambient air on the apparent moments of inertia is usually small but may be as large as 25 percent of the true moments of inertia for airplanes with low wing loading.

The fundamental basis of the effect of the ambient-air mass on bodies undergoing acceleration has been developed in references 1 and 2. References 3, 4, and 5 present experimental data on the effect of the ambient-air mass on the moments of inertia of flat plates obtained by swinging the plates as an integral part of a pendulum. Reference 3 presents a method of correcting the moments of inertia of a full-scale airplane for the ambient-air mass effect by considering the projected areas of various components of the airplane in planes normal and parallel to the plane of symmetry and applying to these projected areas the experimentally determined additional moment-of-inertia corrections for flat plates of finite aspect ratio.

In the present paper, formulas are presented for the rapid evaluation of the additional-mass and moment-of-inertia corrections for airplanes that are swung as an integral part of a pendulum. The method proposed in the preceding reports has generally been conformed to with the exception that the ambient-air mass effect for parts of the airplane such as the fuselage was determined theoretically from the motion of an ellipsoid in a three-dimensional potential flow. The method presented has been applied to 40 complete dynamic airplane models previously tested and the results have been compared with the experimentally determined values.

SYMBOLS

For convenience in defining certain symbols, sketches for identifying dimensional parts of the airplane are given in figures 1 and 2. The numerical values given in these figures are for use in an illustrative example that is subsequently presented.

b span of surface (includes span of fuselage between surface panels; for vertical tail see fig. 2(b))

S area of surface (for wing and horizontal tail includes area of fuselage between surface panels)

A aspect ratio of surface (b^2/S)

c_r root chord of surface

c_t tip chord of surface $\left(\frac{2S}{b} - c_r\right)$

$\bar{c}$ mean chord of surface (S/b)

λ plan-form taper ratio of surface (c_r/c_t)

Γ dihedral of wing or horizontal tail in degrees

L_f length of fuselage (see fig. 1)

w geometric average width of fuselage

d geometric average depth of fuselage

l component in plane of surface of perpendicular distance between axis of rotation and centroid of area of surface

l_{f_X} distance from centroid of side area of fuselage to axis of rotation parallel to and in the plane of the X-axis (conveniently referred to herein as axis of X swinging)

l_{f_Y} component of distance in the X-Y principal plane of fuselage of the perpendicular distance between the centroid of plan area of fuselage and the axis of rotation parallel to and in the plane of the Y-axis

l_{f_Z} distance from centroid of side area of fuselage to axis of rotation parallel to and in the plane of the Z-axis

l_{t_X} distance from centroid of vertical-tail area to axis of rotation parallel to and in the plane of the X-axis

l_{t_Y} component of distance in the X-Y plane of fuselage of the perpendicular distance between the centroid of horizontal-tail area and the axis of rotation parallel to and in the plane of the Y-axis

l_{t_Z} distance from centroid of vertical-tail area to axis of rotation for Z swinging

l_{W_Y} component of distance in the X-Y plane from the centroid of area of wing to axis of rotation parallel to and in the plane of the Y-axis

k coefficient of additional mass of a flat rectangular plate

k' coefficient of additional moment of inertia of a flat rectangular plate

D_λ taper-ratio correction factor

D_Γ dihedral correction factor

k_{fX}, k_{fY}, k_{fZ} coefficients of additional mass of equivalent ellipsoids for motion along the X-, Y-, and Z-axes, respectively

k'_{fX}, k'_{fY}, k'_{fZ} coefficients of additional moments of inertia of equivalent ellipsoids about the X-, Y-, and Z-axes, respectively

m_a additional mass of a body

I_a additional moment of inertia of a body

I_X, I_Y, I_Z moments of inertia about X-, Y-, and Z-body axes, respectively

I_{X_a}, I_{Y_a}, I_{Z_a} total additional moments of inertia about X-, Y-, and Z-body axes, respectively

I_{X_a}', I_{Y_a}', I_{Z_a}' total additional moments of inertia about X, Y, and Z swinging axes, respectively

ρ density of air, slug per cubic foot

Subscripts:

W wing

fus fuselage

ht horizontal tail

vt vertical tail

DEVELOPMENT OF EQUATIONS

Wings and Tail Surfaces

In order to evaluate the additional-mass corrections for the wings and tail surfaces of an airplane it was assumed that these surfaces were flat plates and that the additional-mass corrections previously obtained for flat plates (references 5 and 6) were approximately correct for the wings and tail surfaces. The additional mass of a wing or tail surface in translatory motion may be determined from the following equation:

$$m_a = \frac{\pi\rho}{4} k\bar{c}^2 b \tag{1}$$

where k, the coefficient of additional mass plotted in figure 3 as a function of the aspect ratio, has been obtained by averaging the experimental results of NACA tests presented in reference 5. The values presented in references 3 and 5 for a rectangular wing and those of the present analysis are assumed to be accurate for a tapered wing when considered as an equivalent rectangular wing of chord $\bar{c}$.

The additional moment of inertia of a wing or tail surface rotating about its chord at the midspan is determined from the equation

$$I_a = \frac{\pi\rho}{48} k' \bar{c}^2 b^3 \qquad (2)$$

where k', the coefficient of additional moment of inertia plotted in figure 4 as a function of the aspect ratio of the plate, has been obtained by averaging the experimental results of NACA tests presented in reference 5. Application of correction factors for the effect of dihedral angle and taper ratio gives the following equation:

$$I_a = \frac{\pi\rho}{48} D_\lambda D_\Gamma k' \bar{c}^2 b^3 \qquad (3)$$

The correction factors for the effect of dihedral angle and taper ratio on the values of the additional moments of inertia for flat plates as given in reference 5 are presented in figures 5 and 6.

For rotation about a spanwise axis through the centroid of area of the surface the additional moment of inertia is given by

$$I_a = \frac{\pi\rho}{48} k' \bar{c}^3 b^2 \qquad (4)$$

where the aspect ratio used in determining k' from figure 4 is now $1/A$.

For rotation about an axis displaced from the centroid of area of the surface, the additional moment of inertia about the axis of rotation may be found from the expression

$$I_a' = I_a + m_a l^2$$

where l is the component in the plane of the surface of the perpendicular distance between the axis of rotation and centroid of area of the surface. For example, the additional moment of inertia about an axis parallel to the chord of the surface is given by

$$I_a' = \frac{\pi\rho}{48} k' \bar{c}^2 b^3 + \frac{\pi\rho}{4} k \bar{c}^2 b l^2 \qquad (5)$$

Fuselage

In order to evaluate the additional-mass and moment-of-inertia corrections for the fuselage it may be assumed that the fuselage of an airplane can be approximated in shape by an ellipsoid and that the values of additional mass and additional moments of inertia calculated for the ellipsoid are approximately correct for a fuselage which has the same length and volume as the ellipsoid. That is, the maximum depth and the maximum width of the equivalent ellipsoid are equal, respectively, to $\sqrt{\frac{6}{\pi}}\,d$ and $\sqrt{\frac{6}{\pi}}\,w$ of the fuselage where d and w are values of the average depth and width of the fuselage.

For a fuselage moving in a direction parallel to one of its principal axes in an inviscid fluid, the additional mass is determined from the equations of linear momentum for the equivalent ellipsoid presented in reference 2. For motion along the Y and Z principal axes, the values of the additional mass in terms of the average depth and width of the fuselage are given, respectively, by

$$m_a = \rho k_{fY} L_f w d \tag{6}$$

and

$$m_a = \rho k_{fZ} L_f w d \tag{7}$$

where k_{fY} and k_{fZ}, the coefficients of additional mass for linear motion along the Y- and Z-axes, are presented in figure 7 as a function of the fineness ratio in the plan view and the maximum depth-to-width ratio of the equivalent ellipsoid.

The additional moment of inertia of a fuselage rotating about one of its principal axes is determined from the equations of rotational momentum for the equivalent ellipsoid as presented in references 2 and 6. For rotations about the Y and Z axes, respectively, the additional moments of inertia may be expressed in terms of the average width and depth of the fuselage as

$$I_{Y_a} = \frac{\rho}{5} k'_{fY} L_f wd \left(\frac{L_f^2}{4} + \frac{3d^2}{2\pi}\right) \tag{8}$$

and

$$I_{Z_a} = \frac{\rho}{5} k'_{fZ} L_f wd \left(\frac{L_f^2}{4} + \frac{3w^2}{2\pi}\right) \tag{9}$$

where the coefficients of additional moments of inertia k'_{fY} and k'_{fZ} are presented in figure 8 as a function of the fineness ratio in the plan view and the maximum depth-to-width ratio of the equivalent ellipsoid.

For rotations about reference swinging axes displaced from but parallel, respectively, to the Y and Z principal axes of the fuselage the values of the additional moments of inertia may be obtained from equations (6) to (9) and the moment-of-inertia transference equation

$$I_a' = I_a + m_a l^2$$

as

$$I_{Y_a}' = \frac{\rho}{5} k'_{fY} L_f wd \left(\frac{L_f^2}{4} + \frac{3d^2}{2\pi}\right) + \rho\left(k_{fZ} L_f wd l_{f_Y}^2\right) \tag{10}$$

and

$$I_{Z_a}' = \frac{\rho}{5} k'_{fZ} L_f wd \left(\frac{L_f^2}{4} + \frac{3w^2}{2\pi}\right) + \rho\left(k_{fY} L_f wd l_{f_Z}^2\right) \tag{11}$$

For motion along and rotation about the X principal axis of the airplane, calculations and theory show that the values of the additional mass and additional moments of inertia are relatively small; accordingly, they have not been considered in the following equations for the estimation of the total additional moments of inertia of the airplane about its swinging axes.

Complete Airplane

The evaluation of the additional moments of inertia for a complete airplane entails the applications of equations (1) to (11) to the various portions of the airplane, which can be considered either as flat plates or ellipsoidal bodies. For each part of the airplane the value of the additional moment of inertia is computed about an axis through the centroid of area of the surface and parallel to the corresponding reference swinging axis by applying the appropriate forms of equations (2), (3), (4), (8), and (9). The total values of the additional moments of inertia about the reference swinging axes are then obtained by using the appropriate forms of the moment-of-inertia transference formulae (equations (5), (10), and (11)).

It has been found that, inasmuch as some terms of the resulting general equation for the complete airplane are small, approximate equations for additional moments of inertia about each of the three swinging axes may be written without sacrificing accuracy. These approximate equations are:

$$I_{X_a}' = \frac{\pi\rho}{48}\left(k' D_\lambda D_\Gamma S^2 b\right)_W + \rho\left(k_{fY} L_f w d\, l_{f_X}^{\ 2}\right)_{fus} \tag{12}$$

$$I_{Y_a}' = \left[\frac{\rho}{5} k'_{fY} L_f w d \left(\frac{L_f^{\ 2}}{4} + \frac{3d^2}{2\pi}\right)\right]_{fus} + \rho\left(k_{fZ} L_f w d\, l_{f_Y}^{\ 2}\right)_{fus} + \frac{\pi\rho}{4}\left(k \frac{S^2}{b} l_{t_Y}^{\ 2}\right)_{ht} \tag{13}$$

$$I_{Z_a}' = \left[\frac{\rho}{5} k'_{fZ} L_f w d \left(\frac{L_f^{\ 2}}{4} + \frac{3w^2}{2\pi}\right)\right]_{fus} + \rho\left(k_{fY} L_f w d\, l_{f_Z}^{\ 2}\right)_{fus} + \frac{\pi\rho}{4}\left(k \frac{S^2}{b} l_{t_Z}^{\ 2}\right)_{vt} \tag{14}$$

where, for convenience in making the calculations, S/b is substituted for $\bar{c}$.

An illustration of the application of the procedure to determine the additional moments of inertia is given in the appendix for a typical fighter airplane. The method of determining the various dimensions and areas is indicated on figures 1 and 2. The values of the terms left out of the approximate equations are also given and it may be seen that these terms are negligible.

Comparison of Experimental and Calculated Results

An estimate of the accuracy of the equations (12) to (14) used in calculating the additional moments of inertia may be obtained by inspection of figures 9 to 11 in which the calculated values are plotted against the experimental values which were determined by swinging the models in a vacuum chamber as described in reference 5. The agreement is good since the experimental errors may have been as high as 50 percent of the true values, which were only a small percentage of the total values of the moments of inertia measured with respect to the swinging axes.

A comparison of the experimental values of the total moments of inertia about the body axes with the additional moments of inertia about the axes of rotation is presented in table I. This table indicates that with a swinging gear similar to the arrangement shown in figure 1, the additional moments of inertia probably do not exceed, in the majority of cases, 25 percent of the true moments of inertia about the body axes.

SUMMARY OF RESULTS

Formulas have been developed for the estimation of the additional moments of inertia of airplanes or airplane models. A correlation of the experimental data on 40 models indicates that the satisfactory estimations of the values of the moments of inertia, due to the ambient-air effect, may be determined by means of these formulas.

Langley Memorial Aeronautical Laboratory
National Advisory Committee for Aeronautics
Langley Field, Va., October 15, 1946

APPENDIX

EXAMPLE OF METHOD FOR CALCULATING THE ADDITIONAL MOMENTS OF INERTIA ABOUT THE REFERENCE SWINGING AXES FOR A TYPICAL FIGHTER AIRPLANE

Pertinent data.- In order to illustrate the use of the formulas presented in the text, calculations are presented for a typical fighter airplane. Figure 1 is a sketch of the airplane in position for swinging.

Pertinent coefficients and dimensional data for the airplane are as follows:

Wing:

Area, S, sq ft	220
Span, b, ft	36
Aspect ratio, A	5.9
Mean chord, $\bar{c}$, ft (S/b)	6.1
Component of distance in the X-Y plane from centroid of area of wing to Y-axis of rotation, l_{w_Y}, ft	1.6
Taper ratio, λ	1.66
Dihedral, Γ, deg	3
Additional mass coefficient, k (from fig. 3 for $A = 5.9$)	0.95
Additional moment-of-inertia coefficient, k', for the X swinging (from fig. 4 for $A = 5.9$)	0.88
For the Y swinging, the reciprocal of the aspect ratio $\left(\frac{1}{5.9}\right)$ is used to give an additional moment-of-inertia coefficient k' from figure 4	0.12
Taper-ratio correction, D_{λ} (from fig. 6)	0.86
Dihedral correction, D_{Γ} (from fig. 5)	0.96

Fuselage:

Length, L_f, ft	23.5
Average width, w, ft	3.40
Average depth, d, ft	3.85
Distance from centroid of side area of fuselage to X-axis of rotation, l_{f_X}, ft	7.68
Component of distance in X-Y plane from centroid of top area of fuselage to Y-axis of rotation, l_{f_Y}, ft	4.50

Fuselage - Continued:

Distance from centroid of side area of fuselage to Z-axis of rotation, l_{f_Z}, ft 19.1

Additional moment-of-inertia coefficients obtained from the width-depth ratios and fineness ratio of the fuselage (fig. 7)

k_{fY} 1.04
k_{fZ} 0.86

Additional moment-of-inertia coefficients obtained from the width-depth ratios and fineness ratio of the fuselage (fig. 8)

k'_{fY} 0.89
k'_{fZ} 0.94

Horizontal tail:

Area, S, sq ft 34.7
Span, b, ft 11.5
Aspect ratio, A 3.7
Mean chord, $\bar{c}$, ft (S/b) 3.1
Component of distance in the X-Y plane from centroid of area of horizontal tail to Y-axis of rotation, l_{t_Y} 15.8
Additional mass coefficient, k, (from fig. 3) 0.90
Additional moment-of-inertia coefficient, k', for the X swinging (from fig. 4 for A = 3.7) 0.78
For the Y swinging the reciprocal of the aspect ratio $\left(\frac{1}{3.7}\right)$ is used to give an additional moment-of-inertia coefficient k' from figure 4 . . . . . . 0.18
Taper ratio, λ 1.73
Taper-ratio correction, D_λ (from fig. 6) 0.85

Vertical tail:

Area, S, sq ft 20.2
Span, b, ft 4.6
Aspect ratio, A 1.0
Mean chord, $\bar{c}$, ft (S/b) 4.4
Distance from centroid of area to X-axis of rotation, l_{t_X}, ft 4.3
Distance from centroid of area to Z-axis of rotation, l_{t_Z}, ft 30.6
Additional mass coefficient, k (from fig. 3) 0.59
Additional moment-of-inertia coefficient, k', for the X swinging (from fig. 4 for A = 1.04) 0.41

Vertical tail - Continued:

For the Z swinging the reciprocal of the aspect ratio $\left(\frac{1}{1.04}\right)$ is used to give an additional moment-of-inertia coefficient k from figure 4 . . . . 0.40

Taper ratio, λ 3.0

Taper-ratio correction, D_λ (from fig. 6) 0.72

X-axis.- The additional moment of inertia about the X swinging axis (shown in fig. 1) is obtained from the approximate equation (12) as follows:

$$I_{X_a}' = \frac{\rho\pi}{48}\left(k'D_\lambda D_\Gamma S^2 b\right)_W + \rho\left(k_{fY}L_f w d^2 f_X{}^2\right)_{fus} \tag{A1}$$

Substituting the proper tabulated values in equation (A1) gives

$$I_{X_a}' = \frac{3.14\ (0.002378)}{48}\left[(0.88)(0.86)(0.88)(220)^2(36)\right]_W$$

$$+ \left[(0.002378)(1.04)(23.5)(3.40)(3.85)(7.68)^2\right]_{fus}$$

$$= (185.66)_W + (45)_{fus}$$

$$= 231 \text{ slug-ft}^2 \tag{A2}$$

The value of I_{X_a}' determined experimentally was 269 slug-feet^2.

The exact equation for the additional moments of inertia about the X swinging axis contains the following terms, a numerical evaluation of which gives quantities that are indicative of the relatively small magnitudes of these terms:

$$\frac{\rho\pi}{48}\left(k'D_\lambda D_\Gamma S^2 b\right)_{ht}$$

$$= \left[\frac{3.14(0.002378)}{48}(0.78)(0.85)(1)(34.7)^2(11.5)\right]_{ht}$$

$$= 1.47 \text{ slug-ft}^2 \tag{A3}$$

$$\frac{\rho\pi}{48}\left(k'D_{\lambda}S^{2}b\right)_{vt}$$

$$= \left[\frac{3.14(0.002378)}{48}(0.41)(0.72)(20.2)^{2}(4.6)\right]_{vt}$$

$$= 0.089 \text{ slug-ft}^{2} \tag{A4}$$

$$\frac{\rho\pi}{4}\left(k\frac{S^{2}}{b}\,l_{t_X}{}^{2}\right)_{vt}$$

$$= \left[\frac{3.14(0.002378)}{4}(0.59)\frac{(20.2)^{2}}{4.6}(4.3)^{2}\right]_{vt}$$

$$= 1.81 \text{ slug-ft}^{2} \tag{A5}$$

Y-axis.- The additional moment of inertia about the Y swinging axis (shown in fig. 1) is obtained from the approximate equation (13) as follows:

$$I_{Y_a}{}' = \left[\frac{\rho}{5}k'_{fY}L_f v d\left(\frac{L_f{}^{2}}{4}+\frac{3d^{2}}{2\pi}\right)\right]_{fus} + \left[\rho\left(k_{fZ}L_f v d\, l_{f_Y}{}^{2}\right)\right]_{fus}$$

$$+ \left[\frac{\rho\pi}{4}\left(k\frac{S^{2}}{b}\,l_{t_Y}{}^{2}\right)\right]_{ht} \tag{A6}$$

Substituting the proper tabulated values in equation (A6) gives

$$I_{Y_a}{}' = \left\{\frac{0.002378}{5}(0.89)(23.5)(3.40)(3.85)\left[\frac{(23.5)^{2}}{4}+\frac{3}{6.28}(3.85)^{2}\right]\right\}_{fus}$$

$$+ \left[(0.002378)(0.86)(23.5)(3.40)(3.85)(4.50)^{2}\right]_{fus}$$

$$+ \left\{\frac{3.14(0.002378)}{4}\left[\frac{0.90(34.7)^{2}}{11.5}(15.8)^{2}\right]\right\}_{ht}$$

$$= (18.90)_{fus} + (12.74)_{fus} + (43.99)_{ht}$$

$$= 76 \text{ slug-ft}^2 \tag{A7}$$

The value of $I_{Y_a}{}'$ determined experimentally was 143 slug-feet^2.

The exact equation for the additional moments of inertia about the Y swinging axis contains the following terms, a numerical evaluation of which gives quantities that are indicative of the relatively small magnitudes of these terms:

$$\frac{\rho\pi}{48}\left(k'D_\lambda D_i S^2 c\right)_W$$

$$= \left[\frac{3.14(0.002378)}{48}(0.12)(0.86)(0.96)(220)^2(6.1)\right]$$

$$= 4.56 \text{ slug-ft}^2 \tag{A8}$$

$$\frac{\rho\pi}{4}\left(k\frac{S^2}{b}l_{W_Y}{}^2\right)_W = \left\{\frac{3.14(0.002378)}{4}\left[\frac{0.95(220)^2}{36}(1.6)^2\right]\right\}_W$$

$$= 6.11 \text{ slug-ft}^2 \tag{A9}$$

$$\frac{\rho\pi}{48}\left(k'D_\lambda D_i S^2 c\right)_{ht}$$

$$= \left[\frac{3.14(0.002378)}{48}(0.18)(0.85)(1)(34.7)^2(3.1)\right]_{ht}$$

$$= 0.089 \text{ slug-ft}^2 \tag{A10}$$

Z-axis.- The additional moment of inertia about the Z swinging axis (shown in fig. 1) is obtained from the approximate equation (14) as follows:

$$I_{Z_a}' = \left[\frac{\rho}{5} k'_{fZ} L_f w d \left(\frac{L_f^2}{4} + \frac{3w^2}{2\pi}\right)\right]_{fus} + \left[\rho\left(k_{fY} L_f w d\ l_{f_Z}{}^2\right)\right]_{fus}$$

$$+ \left[\frac{\rho\pi}{4}\left(k\ \frac{S^2}{b}\ l_{t_Z}{}^2\right)\right]_{vt} \tag{A11}$$

Substituting the proper tabulated values in equation (A11) gives

$$I_{Z_a}' = \left\{\frac{(0.002378)}{5}(0.94)(23.5)(3.4)(3.85)\left[\frac{(23.5)^2}{4} + \frac{3}{6.28}(3.4)^2\right]\right\}_{fus}$$

$$+ \left[(0.002378)(1.04)(23.5)(3.4)(3.85)(19.1)^2\right]_{fus}$$

$$+ \left\{\frac{3.14(0.002378)}{4}\left[\frac{0.59(20.2)^2}{4.6}(30.6)^2\right]\right\}_{vt}$$

$$= (19.70)_{fus} + (277.65)_{fus} + (91.63)_{vt}$$

$$= 389 \text{ slug-ft}^2 \tag{A12}$$

The value of I_{Z_a}' determined experimentally was 346 slug-feet^2.

The exact equation for the additional moments of inertia about the Z swinging axis contains the following term, a numerical evaluation of which gives a quantity that is indicative of the relatively small magnitude of this term:

$$\frac{\rho\pi}{48}\left(k' D_\lambda S^2 \bar{c}\right)_{vt}$$

$$= \left[\frac{3.14(0.002378)}{48}(0.41)(0.72)(20.2)^2(4.4)\right]_{vt}$$

$$= 0.083 \text{ slug-ft}^2 \tag{A13}$$

REFERENCES

1. Green, George: Researches on the Vibration of Pendulums in Fluid Media. Trans. Roy. Soc. Edinburg, vol. 13, 1836, pp. 54-62.

2. Lamb, Horace: Hydrodynamics. Sixth ed., Cambridge Univ. Press, 1932, pp. 1[illegible]-155.

3. Soulé, Hartley A., and Miller, Marvel P.: The Experimental Determination of the Moments of Inertia of Airplanes. NACA Rep. No. 467, 1933.

4. Pleines, W.: Der Einfluss der mitschwingenden Luftmassen bei Pendelschwingungsversuchen mit Flugzeugen. Jahrb. 1937 der deutschen Luftfahrtforschung, R. Oldenbourg (Munich), pp. I 595-I 602.

5. Gracey, William: The Additional-Mass Effect of Plates as Determined by Experiments. NACA Rep. No. 707, 1941.

6. Munk, Max M.: Fluid Mechanics. Pt. II, Vol. I of Aerodynamic Theory, div. C, ch. III - VII, W. F. Durand, ed., Julius Springer (Berlin), 1934, pp. 241-292.

TABLE I.- COMPARISON OF THE EXPERIMENTAL TOTAL VALUES OF THE MOMENTS OF INERTIA ABOUT THE BODY AXES AND THE ADDITIONAL MOMENTS OF INERTIA ABOUT THE AXIS OF ROTATION OF THE COMPOUND PENDULUM OF 40 FREE-SPINNING AIRPLANE MODELS

[Values are in gr-in.^{2}]

Airplane model	Model scale	I_X	I_{X_a}'	I_Y	I_{Y_a}'	I_Z	I_{Z_a}'
XSB2U-1	1/16	6,520	1160	14,082	398	19,217	2088
BT-9	1/16	5,280	717	7,452	344	11,260	1270
P-35	1/18	3,195	300	4,681	160	7,095	385
XOS2U-1	1/16	4,044	877	10,190	859	13,234	1849
P-36A	1/20	1,327	232	2,937	79	3,962	482
XSO2U-1	1/16	5,188	890	16,369	540	20,361	2337
YFM-1	1/25	8,514	1128	4,902	639	12,556	1894
XSO3C-1	1/14	11,566	1385	34,169	1291	41,896	3309
XSB2A-1	1/25	1,908	246	4,417	150	6,115	445
B-26	1/26	11,266	523	12,354	651	22,899	1601
XP-46	1/20	2,158	166	3,640	116	5,617	395
XTBU-1	1/24	3,311	350	6,328	119	9,216	579
XP-47B	1/20	9,111	387	8,572	244	16,978	656
XP-67	1/27	6,156	183	3,752	63	9,327	415
XSB3C-1	1/20.83	8,694	831	11,232	729	19,008	826
XP-69	1/20	17,375	1181	32,307	735	48,451	2153
XP-62	1/22	5,402	432	9,198	233	13,755	843
XF14C-1	1/20	7,695	695	9,686	368	15,990	1694
XF2A-1	1/16	4,578	436	7,452	503	11,250	875
A-17	1/15	17,190	2100	21,265	730	34,464	2233
XF4F-2	1/12	12,730	2540	31,149	1725	41,006	2740
NF-1	1/12	16,289	1700	32,882	1308	48,098	2830
XF4U-1	1/20	4,862	383	5,303	268	9,474	779
XF5F-1	1/22	4,401	299	2,927	102	7,044	313
XPT-12	1/14	9,744	1320	16,305	601	24,606	1603
XBT-11	1/16	5,416	876	8,746	335	11,835	1202
XP-50	1/25	2,965	98	1,630	99	4,560	122
XTBF-1	1/22	4,793	857	8,632	386	12,722	958
P-39D	1/20	3,417	137	3,992	90	7,032	432
P-30	1/16	7,944	738	14,511	180	20,301	1550
P-40F	1/20	3,304	274	5,190	82	7,980	465
SNC-1	1/14	4,856	659	11,194	491	15,394	1246
XSB2D-1	1/20	9,155	566	16,775	463	24,856	1601
XA-39	1/20	13,915	1529	17,542	1156	30,136	2195
XP-75	1/16	20,309	1745	33,701	1089	51,829	3814
XP-71	1/28	18,930	653	12,860	370	31,790	3241
DC-3	1/23.75	18,554	2764	25,517	870	41,856	2461
XCG-16	1/32	2.821	707	2,043	150	4,688	752
XC-82	1/60	770	167	373	144	1,119	45
SBN-1	1/18	3,587	428	6,601	239	9,741	867

NATIONAL ADVISORY
COMMITTEE FOR AERONAUTICS

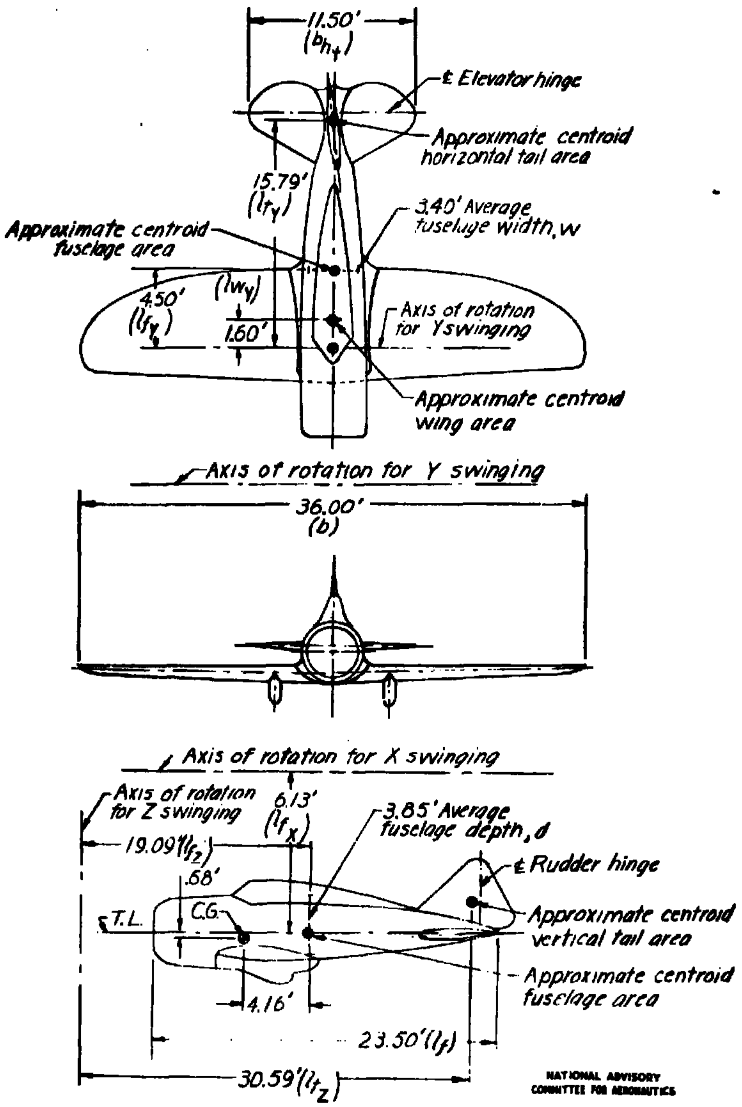

Figure 1.- Sketch of a typical model showing dimensions necessary for the calculation of the additional moments of inertia. All dimensions are full-scale values.

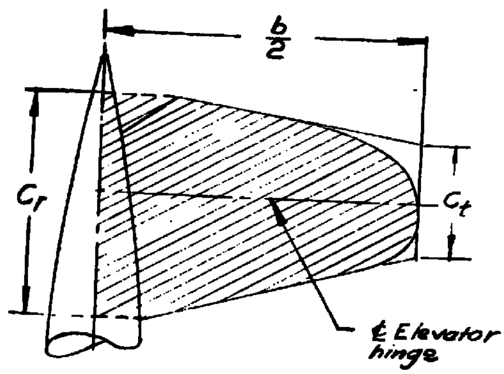

(a) Horizontal tail.

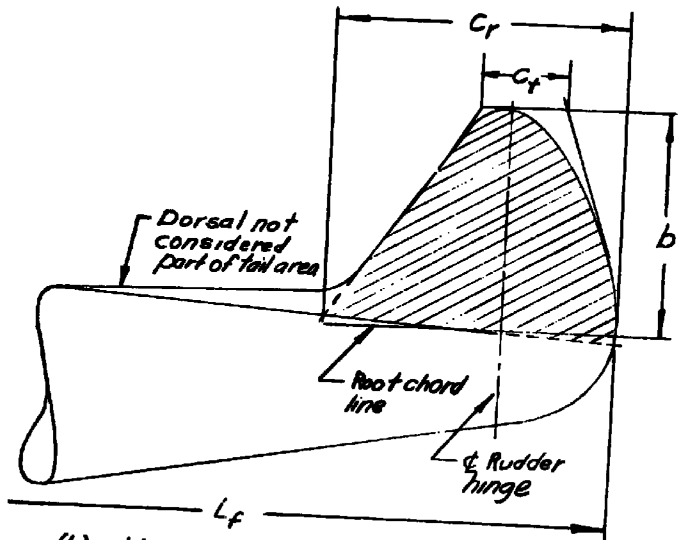

(b) Vertical Tail.

NATIONAL ADVISORY
COMMITTEE FOR AERONAUTICS

Figure 2.- Sketch illustrating method of measuring the chords, span, and area of the horizontal and vertical tail surfaces; $c_t = \left(\frac{2S}{b}\right) - c_r$ where S is the area of the tail surfaces.

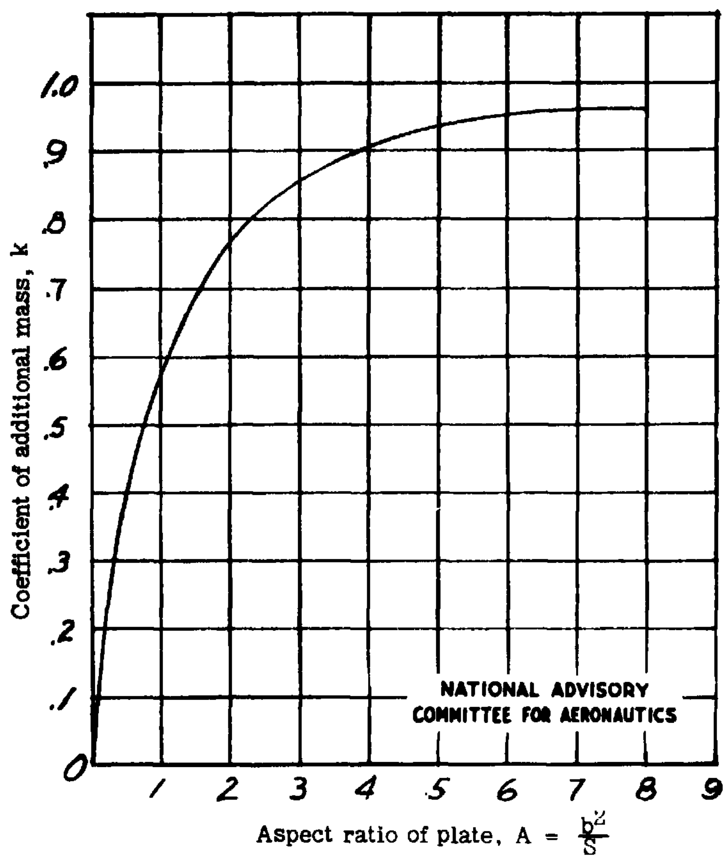

Figure 3.- Coefficients of additional mass for rectangular plates. Curve is average of NACA 1933 and 1940 tests. (Reference 5)

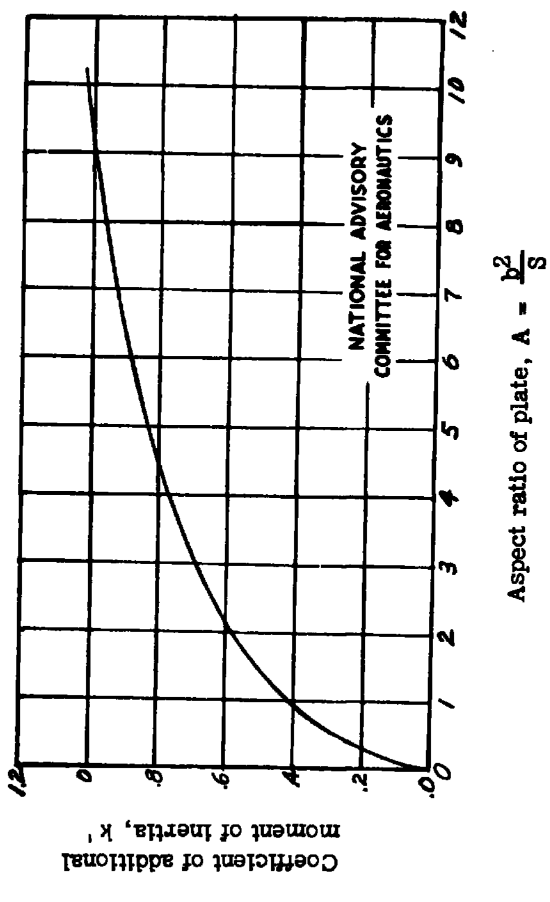

Figure 4.- Coefficients of additional moment of inertia for rectangular plates. Curve is average of NACA 1933 and 1940 tests. (Reference 5)

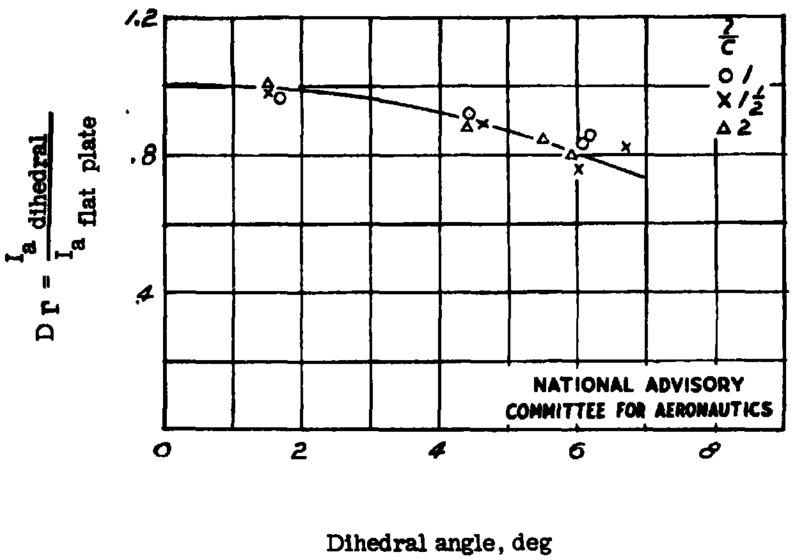

Figure 5.- Variation of the additional moments of inertia of a single plate with dihedral angle; A = 4 (reference 5).

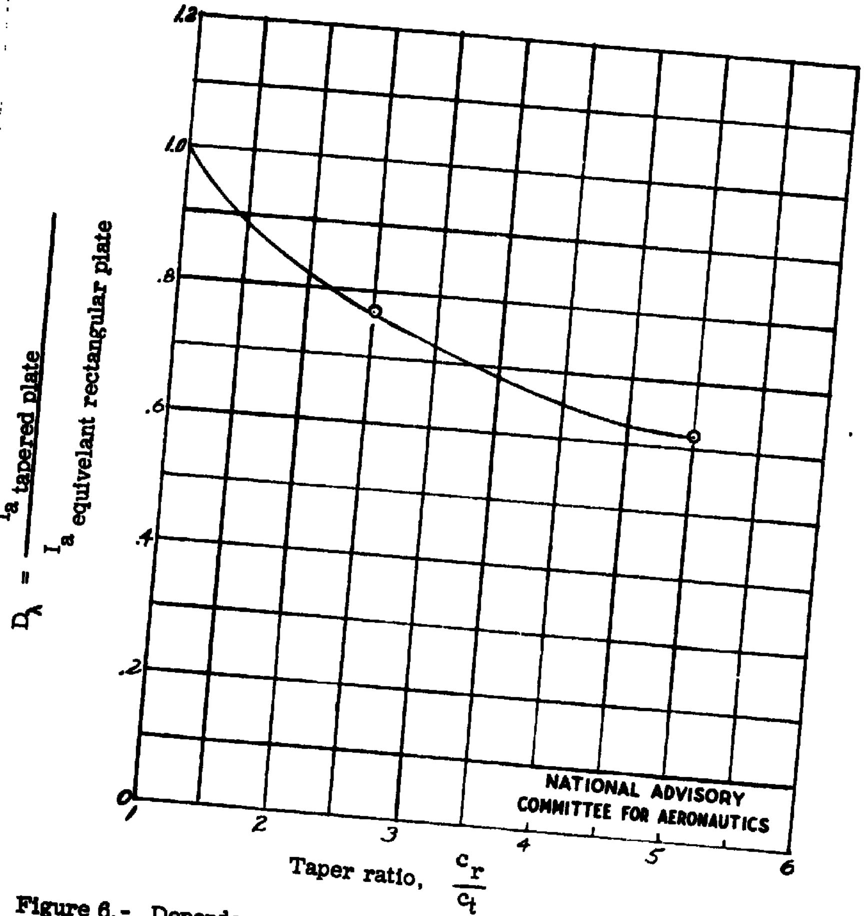

Figure 6.- Dependence of the additional moment of inertia on taper ratio (reference 5).

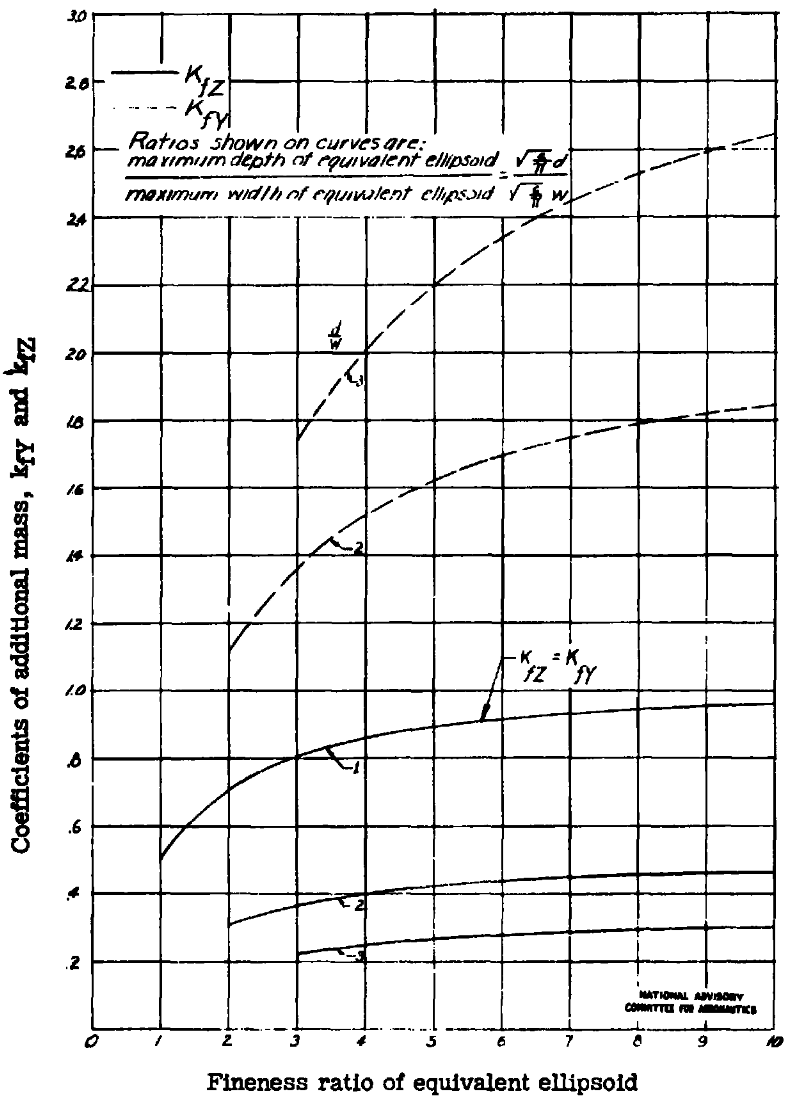

Figure 7.- The variation of the coefficients of additional mass k_{fY} and k_{fZ} with the fineness ratio of an equivalent ellipsoid

$$\frac{\text{Actual length}}{\text{Maximum width}} = \frac{L_f}{w\sqrt{\frac{6}{\pi}}}.$$

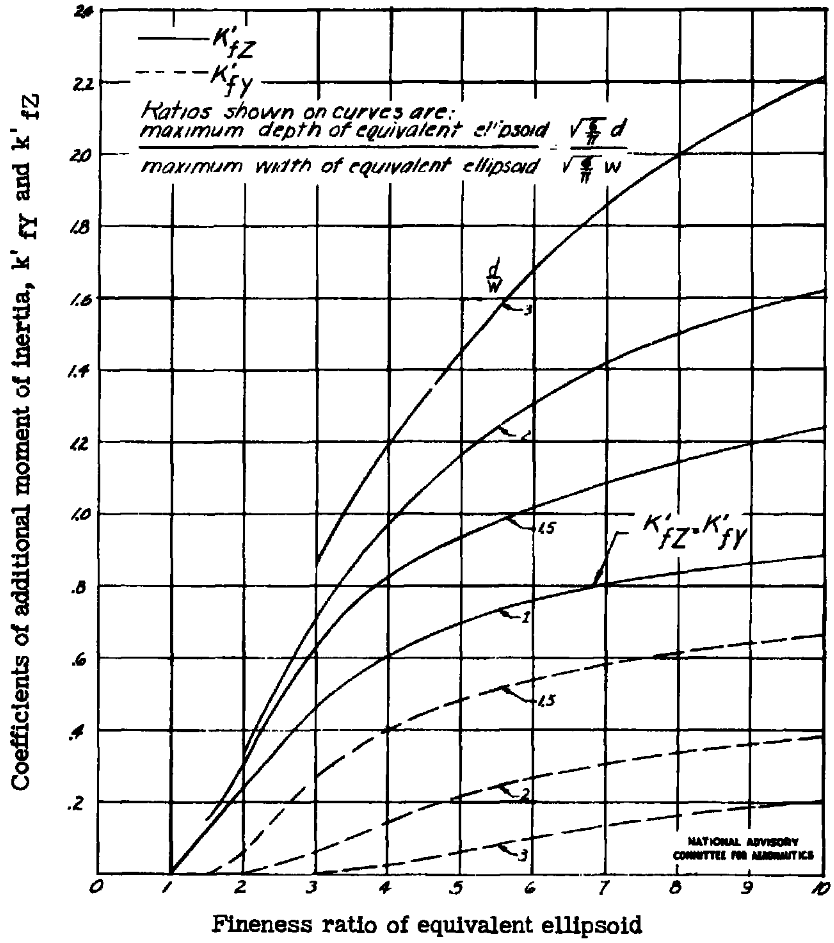

Figure 8.- The variation of the coefficients of additional moment of inertia k'_{fZ} and k'_{fY} with fineness ratio of an equivalent ellipsoid $\frac{\text{Actual length}}{\text{Maximum width}} = \frac{L_f}{w\sqrt{\frac{6}{\pi}}}$.

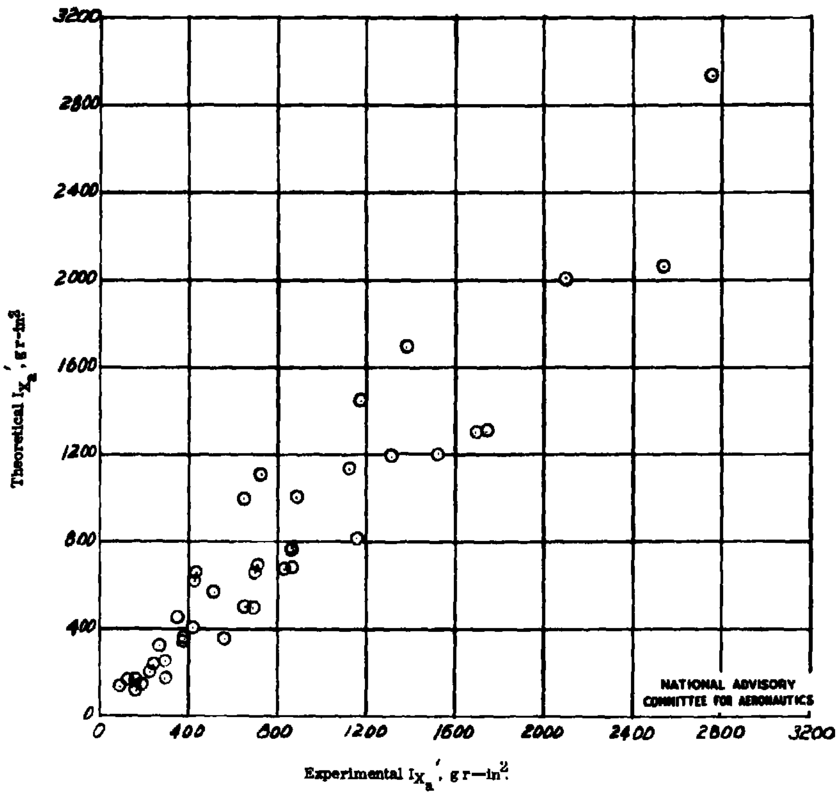

Figure 9.- Comparison of the experimental and calculated model values of the additional moments of inertia about the X swinging axis for 40 free-spinning models.

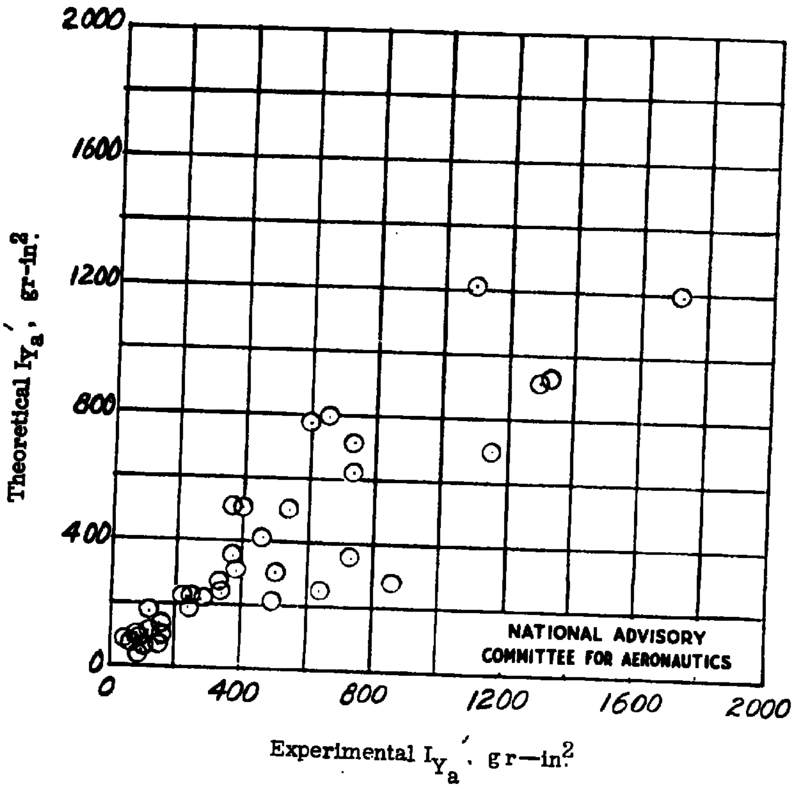

Figure 10.- Comparison of the experimental and calculated model values of the additional moments of inertia about the Y-swinging axis for 40 free-spinning models.

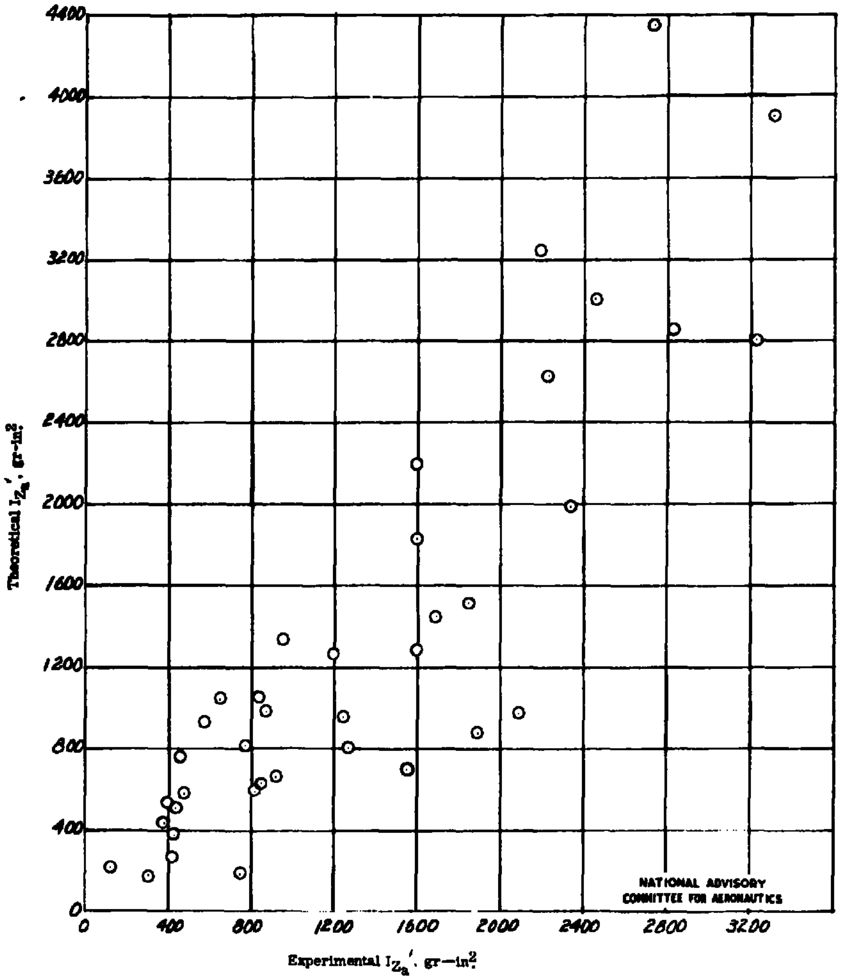

Figure 11.- Comparison of the experimental and calculated model values of the additional moments of inertia about the Z swinging axis for 40 free-spinning models.

REEL – C

204

A.T.I.

7241

TITLE: Formulas for Additional Mass Corrections to the Momeots of Inertia of Airplanes	ATI- 7241
	REVISION (None)
AUTHOR(S): Malvestuto, F.; Gale, L. J.	ORIG. AGENCY NO. TN-1187
ORIGINATING AGENCY: National Advisory Committee for Aeronautics, Washington, D. C.	PUBLISHING AGENCY NO.
PUBLISHED BY: (Same)	

DATE	DOC. CLASS.	COUNTRY	LANGUAGE	PAGES	ILLUSTRATIONS
Feb '47	Unclass.	U. S.	Eng.	28	tables, diagrs, graphs

ABSTRACT:

Formulas are preseoted to obtain true momeots of inertia of airplanes from experimental momeots. A correlation of additional moments of ioertia calculated by these formulas with experimental additional moments obtaioed from tests on forty models indicates that satisfactory estimations of additional moments can be determined. For eacb part of airplane, the value of moment is computed about an axis through ceotroid of surface area and parallel to correspooding reference swinging axis by applying appropriate form of equations.

DISTRIBUTION: Request copies of this report only from Originating Agency

DIVISION: Aerodynamics (2) SECTION: Stability and Cootrol (1) ATI SHEET NO.: R-2-1-38	SUBJECT HEADINGS: Airplanes - Moments of inertia (08473.5)